Integrated Direct Optimization of Structure/Regulator/Observer for Large Flexible Spacecraft

Junjiro Onoda* and Naoyuki Watanabe†
Institute of Space and Astronautical Science, Kanagawa, Japan

A direct numerical optimization approach for the design of an optimal controller, composed of a regulator and an observer, is proposed for the integrated structure/controller optimization of flexible spacecraft. Since the approach takes into account the uncontrolled residual modes, it will not only optimize them, based on an actual performance index affected by the residual modes, but will also suppress the spillover instability. The approach is applied to the design of a controller for a simple supported beam, and the characteristics of the resulting system are investigated. The example demonstrates that the resulting controller is stable even when the linear quadratic Gaussian (LQG) controller is unstable. Insensitivity of the resulting system to parameter variations is also demonstrated in comparison with the LQG controller. The approach is subsequently incorporated into a structure/controller simultaneous optimization scheme and applied to the design of a beam-like flexible spacecraft. The results demonstrate the effectiveness of the proposed approach, the importance of taking into account the effects of the residual modes, and the advantage of the simultaneous optimization.

Introduction

THE vibration suppression of a flexible space structure is an important and difficult problem. One of the most attractive solutions to this problem is active vibration control by using the attitude control system. Traditionally, the structure and the attitude control system of a spacecraft are designed separately. However, because of the very strong interaction between a structure and a control system in active vibration control, simultaneous optimization of both systems may be necessary in order to obtain the maximum performance with minimum cost. Recently, many works on the simultaneous optimization of the structure and control system have been published using various objective functions and constraints.[1-9]

In many of these works, the state feedback control is adopted, but most of them assume a "perfect knowledge" about the state, even though the state has to be reconstructed from the sensor signals by an observer in the actual situation. Furthermore, the truncated "residual modes" are not taken into account. These assumptions preclude the degrading effect of the residual modes on the performance, especially the possibility of the spillover instability[10] from the mathematical model, and therefore, may lead to erroneous conclusions. These simultaneous optimization approaches need to be improved by including both the observer and residual modes (i.e., the possibility of the spillover instability) in the mathematical model.

A possible approach, which solves this problem, is to numerically search the optimal parameter values of the structure and of the controller by minimizing the objective function involving the effect of the residual modes. The advantages of this approach are that the effects of the residual modes can be easily taken into the account and that various constraints can be flexibly imposed, since it is a numerical approach. A major defect of this approach is the large number of computations required for the nonlinear optimization with the constraints. However, this defect may be diluted when it is incorporated with the structural optimization, for which a numerical nonlinear optimization is necessary regardless of the choice of the controller design approach. In the present paper, this integrated direct optimization approach is proposed. Because the characteristics of the controller designed by the direct optimization are not well known, the approach is first applied to the design of a controller in order to investigate the characteristics of the resulting system. Then, it is incorporated into the integrated optimization of the structure and controller. The integrated approach is demonstrated by a beam-like spacecraft example.

Received Feb. 6, 1989; presented as Paper 89-1313 at the AIAA/ASME/ASCE/AHS/ASC 30th Structures, Structural Dynamics, and Materials Conference, Mobile, AL, April 3-5, 1989; revision received Sept. 13, 1989.

*Associate Professor. Member AIAA.
†Research Associate.

Optimization of Regulator and Observer

Before proceeding to the structure/regulator/observer simultaneous optimization, let us first consider the design of the controller (composed of a regulator and an observer) for the following system, which will allow us to investigate the characteristics of a controller designed by the direct optimization approach.

$$\dot{x}_1 = A_1 x_1 + B_1 u + w_{11} \tag{1}$$

$$\dot{x}_2 = A_2 x_2 + B_2 u + w_{12} \tag{2}$$

$$y = C_1 x_1 + C_2 x_2 + w_2 \tag{3}$$

$$\dot{\hat{x}}_1 = A_1 \hat{x}_1 + B_1 u + K(y - C_1 \hat{x}_1) \tag{4}$$

$$u = -G\hat{x}_1 \tag{5}$$

where

x_1 = state vector of controlled modes
x_2 = state vector of residual modes
A_1, A_2 = plant matrices
B_1, B_2 = input matrices
C_1, C_2 = observation matrices
$\hat{x}_1$ = reconstructed controlled modes state vector
u = control force vector
y = observed variables vector
w_{11}, w_{12}, w_2 = white noise vector
G = regulator gain matrix
K = observer gain matrix

The dynamics of the structure is assumed to be sufficiently represented by the n_1 controlled modes and the n_2 residual modes. The other (usually higher order) modes are assumed to be negligible. It should be noted that the regulator feeds back the state of the controlled modes only. The modal parameters of the controlled modes and the residual modes are assumed to be known.

Here, we define the following performance index

$$J_1 \equiv \gamma + C_E \tag{6}$$

where

$$\gamma \equiv E[x_1^T Q_{11} x_1 + x_1^T Q_{12} x_2 + x_2^T Q_{12}^T x_1 + x_2^T Q_{22} x_2] \tag{7}$$

$$C_E \equiv E[u^T R u] \tag{8}$$

and

γ = response index

C_E = control effort index

Q_{ij}, R = weighting matrices

$E[\ ]$ = expectation operator

The proposed direct optimization approach for the design of a controller is to find G and K, which minimize J_1. The definition of the response index γ is reasonable because it includes the effects of the residual modes. The total controlled system, involving the residual modes, is stable if the resulting value of J_1 is finite. The well-established linear quadratic Gaussian (LQG) design method cannot be used directly to minimize J_1 because of the residual modes. Concerning the regulator gain design, Kosut[11] obtained the optimality equations based on a similar objective function. However, they are quite formidable, as he has also stated. In this paper, J_1 is numerically minimized by the NEWSUMT-A computer program.[12]

The value of J_1 can be estimated as[13]

$$J_1 = \mathrm{tr}[PV] \tag{9}$$

where P is the solution of

$$PA + A^T P + Q = 0 \tag{10}$$

and

$$V\delta(\tau) \equiv \begin{pmatrix} V_{11} & V_{12} & 0 \\ V_{12}^T & V_{22} & 0 \\ 0 & 0 & V_2 \end{pmatrix} \delta(\tau)$$

$$= E\{w_{11}(t)^T, w_{12}(t)^T, w_2(t)^T K^T)^T \times [(w_{11}(t-\tau)^T, w_{12}(t-\tau)^T, w_2(t-\tau)^T K^T]\} \tag{11}$$

$$Q \equiv \begin{pmatrix} Q_{11} & Q_{12} & 0 \\ Q_{12}^T & Q_{22} & 0 \\ 0 & 0 & G^T R G \end{pmatrix} \tag{12}$$

$$A \equiv \begin{pmatrix} A_1 & 0 & -B_1 G \\ 0 & A_2 & -B_2 G \\ KC_1 & KC_2 & A_1 - B_1 G - KC_1 \end{pmatrix} \tag{13}$$

where $\delta(\tau)$ = Dirac's delta function. No correlation between w_2 and other noises are assumed.

In all of the subsequent numerical examples of both the simply supported beam and the free-free beam, the initial values of the regulator and observer gains are the LQG control gains. When the closed-loop system is unstable, the value of J_1 diverges. Therefore, when the initial values make the system unstable, the maximum value of the real parts of the eigenvalues of A

$$r \equiv \max[\mathrm{Re}(\lambda_i)] \tag{14}$$

where λ_i is the ith eigenvalues of A

is minimized first, and, subsequently, the optimization that minimizes J_1 is carried out. Recall, n_1 and n_2 represent the number of controlled modes and residual modes, respectively. The controlled modes are the lowest modes and the residual modes, which are taken into account in the present approach, are the next lowest modes after the controlled modes.

Sometimes designers want to make the value of r less than a certain negative value r^* in order to guarantee a certain amount of damping in all of the modes. For this purpose, a constraint

$$g_1 \equiv r^* - r \geq 0 \tag{15}$$

can easily be incorporated in the direct numerical optimization scheme. In some cases, however, it may be difficult to force the real parts of some eigenvalues to be less than r^* because, for example, the residual modes are not directly controlled by the controller and are only affected by them through the spillover. In such cases, the constraint [Eq. (15)] may result in a considerable penalty in the performance index J_1. Another attractive approach is to decrease only the real parts of the eigenvalues, which can easily be done without substantially increasing J_1. This approach can be implemented by replacing the objective function with the following modified function:

$$J_1' = \left\{1 + \epsilon \sum_i h[\mathrm{Re}(\lambda_i) - r^*]\right\} J_1 \tag{16}$$

where

$$h[z] = \begin{cases} z & \text{if } z \geq 0 \\ 0 & \text{if } z < 0 \end{cases} \tag{17}$$

Furthermore, it is also possible to take into account the ambiguity of the controlled structure.[14] The overall flexibility of the present method is an advantage for the direct numerical approach.

Simply Supported Beam Example

In order to demonstrate the present optimization method and to evaluate the characteristics of the solutions, a control of a simply supported beam, shown in Fig. 1, is investigated. This problem is also investigated by Balas[10] and Czajkowski et al.[15] The beam has a transverse displacement sensor and an actuator that generates the transverse force u as shown in the figure. The length, the mass, and the bending stiffness of the beam are unity. In the following simply supported beam

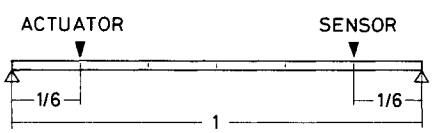

Fig. 1 Simply supported beam.

examples, the state vectors are defined as follows:

$$x_1 = \lfloor q_1,\ldots,q_n,\dot{q}_1/\omega_1,\ldots,\dot{q}_{n_1}/\omega_{n_1} \rfloor^T$$

$$x_2 = \lfloor q_{n_1+1},\ldots,q_{n_1+n_2},\dot{q}_{n_1+1}/\omega_{n_1+1},\ldots,\dot{q}_{n_1+n_2}/\omega_{n_1+n_2} \rfloor^T \tag{18}$$

where q_i denotes the modal displacement associated with the ith mode, $\sqrt{2}\sin(i\pi X)$, ω_i is the angular frequency of the ith mode, and X is the coordinate along the beam with the origin at the left end. The parameter values used in the following simply supported beam examples are listed in Table 1, where ζ is the structural damping ratio of all of the modes.

If there are no residual modes (i.e., $n_2 = 0$), the objective function of the present approach is identical with that of the LQG approach. Therefore, to check if the present method actually leads to the same results as the LQG approach, both the present approach and the LQG approach are first applied to case A, which has no residual modes. The results are compared in Table 2, showing that the present approach can produce the identical configuration as the LQG approach. However, there are other optimal configurations that minimize J_1, resulting in the identical value. The eigenvalues of the entire system of each optimal configuration are identical with those of other optimal configurations, although the eigenval-

Table 1 Parameter values of simply supported beam examples

	Case A	Case B	Case C
n_1	2	3	3
n_2	0	1	1
Q_{11}	Ω_1[a]	Ω_1	Ω_1
Q_{12}	0	0	0
Q_{22}	—	Ω_2[b]	Ω_2
V_{11}	I	Ω_1	Ω_1
V_{12}	—	0	0
V_{22}	—	0	0
V_2	0.1	1	1
ζ	10^{-5}	10^{-4}	10^{-4}
R	1	0.2	3.0

[a] $\Omega_1 = \text{diag}\,(\omega_1^2,\ldots,\omega_{n_1}^2,\ \omega_1^2,\ldots,\omega_{n_1}^2)$.
[b] $\Omega_2 = \text{diag}\,(\omega_{n_1+1}^2,\ldots,\omega_{n_1+n_2}^2,\ \omega_{n_1+1}^2,\ldots,\omega_{n_1+n_2}^2)$.

Table 3 Increment of normalized performance index ($\Delta J_1/J_L$) due to ±10% parameter variations

	Example A1	Example A2	Examples A3 & A4
Original value	1.2278	1.2278	1.2278
Parameter			
A1(3,1)	0.0072	0.0072	0.0072
A1(4,2)	0.2374	0.2377	0.2374
B1(3,1)	0.0108	0.0108	0.0108
B1(4,1)	0.1003	0.1003	0.1003
C1(1,3)	0.0026	0.0026	0.0026
C1(1,4)	0.0264	0.0264	0.0264
G(1,1)	0.0	0.0	0.0
G(1,2)	0.0	0.0	0.0
G(1,3)	0.0002	0.0006	0.0006
G(1,4)	0.0012	0.0012	0.0050
K(1,1)	0.0006	0.0002	0.0002
K(2,1)	0.0050	0.0050	0.0012
K(3,1)	0.0	0.0	0.0
K(4,1)	0.0	0.0001	0.0

Table 2 Initial gain values, final optimal gains, eigenvalues, and performance index of case A example

		Example A1	Example A2	Example A3	Example A4
Initial gain values	G	0.0	0.5	0.5	
		0.0	0.5	0.5	
		0.0	0.5	0.5	
		0.0	0.5	0.5	LQG
	K	0.0	0.0	0.5	DESIGN
		0.0	0.0	0.5	
		0.0	0.0	0.5	
Final gain values	G	1.870	−0.185	0.095	0.095
		−20.93	−9.387	−1.059	−1.059
		44.10	9.920	9.866	9.866
		−175.8	−175.8	−39.44	−39.44
	K	1.000	4.436	4.468	4.468
		0.999	0.998	4.440	4.440
		0.096	0.314	0.189	0.189
		0.027	0.092	0.530	0.530
Regulator eigenvalues		−1.567 ±j9.869	−0.353 ±j9.870	−0.353 ±j9.870	−0.353 ±j9.870
		−2.732 ±j39.48	−2.729 ±j39.48	−0.612 ±j39.48	−0.612 ±j39.48
Observer eigenvalues		−0.353 ±j9.870	−1.567 ±j9.869	−1.567 ±j9.869	−1.567 ±j9.869
		−0.612 ±j39.48	−0.612 ±j39.48	−2.732 ±j39.48	−2.732 ±j39.48
Performance index, J_1		3463.13	3463.13	3463.13	3463.13

Table 4 Gains, eigenvalues, and normalized performance index of case B examples

Example B1 (reduced-order LQG)	Example B2 (present method)	Example B3 (present method)
Gains $G = \lfloor 0.3875, -3.548, 12.85, 22.04, -87.95, 197.1 \rfloor$ $K = \lfloor 9.754, 39.41, 68.42, -1.470, -2.076, 56.60 \rfloor^T$ System eigenvalues $-0.790 \pm j9.868$ $-2.019 \pm j9.900$ $-1.369 \pm j39.49$ $-14.23 \pm j41.43$ $-1.580 \pm j88.81$ $-59.79 \pm j84.32$ $0.039 \pm j157.5$ $J_1/J_L = \infty$	Gains $G = \lfloor -16.22, -4.115, 13.40, 24.01, -84.21, 197.7 \rfloor$ $K = \lfloor 39.27, 38.45, 26.53, -41.55, 36.30, 53.41 \rfloor^T$ System eigenvalues $-1.032 \pm j9.245$ $-0.0020, -11.9$ $-1.296 \pm j39.51$ $-13.41 \pm j47.92$ $-1.580 \pm j88.81$ $-37.35 \pm j105.7$ $-0.104 \pm j157.6$ $J_1/J_L = 1.0614$	Gains $G = \lfloor -16.11, -2.459, 12.88, 16.71, -85.79, 197.4 \rfloor$ $K = \lfloor 168.9, 27.50, 2.228, -18.51, 79.45, 77.55 \rfloor^T$ System eigenvalues $-0.609 \pm j9.270$ $-3.051, -44.05$ $-1.324 \pm j39.48$ $-14.09 \pm j45.74$ $-1.580 \pm j88.81$ $-40.41 \pm j107.8$ $-0.110 \pm j157.6$ $J_1/J_L = 1.0613$
Example B4 [present method with Eq. (15)]	**Example B5 [present method with Eq. (16)]**	**Example B6 (full-order LQG)**
Gains $G = \lfloor -11.42, -15.70, 16.71, 63.23, -99.04, 188.1 \rfloor$ $K = \lfloor 3.451, 35.34, 12.50, -2.279, 16.49, 67.46 \rfloor^T$ System eigenvalues $-2.273 \pm j9.238$ $-0.500 \pm j9.604$ $-1.539 \pm j39.54$ $-9.039 \pm j43.45$ $-1.507 \pm j88.78$ $-21.68 \pm j124.7$ $-0.500 \pm j157.3$ $J_1/J_L = 1.084$	Gains $G = \lfloor -12.43, -35.22, 40.35, 191.6, -84.35, 194.3 \rfloor$ $K = 12.58, 71.05, -1.684, -7.941, 70.12, 78.10 \rfloor^T$ System eigenvalues $-1.000, -12.95$ $-1.071 \pm j9.308$ $-1.263 \pm j39.56$ $-15.47 \pm j52.34$ $-1.553 \pm j88.82$ $-29.90 \pm j129.4$ $-0.301 \pm j157.5$ $J_1/J_L = 1.064$	Gains $G = \lfloor 0.364, -3.15, 10.1, -21.6 22.0, -88.0, 197, -348. \rfloor$ $K = \lfloor 9.75, 39.4, 68.4, 0.0, -1.47, -2.08, 56.6, 0.0 \rfloor^T$ System eigenvalues $-0.789 \pm j9.870$ $-2.026 \pm j9.897$ $-1.368 \pm j39.48$ $-14.33 \pm j41.61$ $-1.580 \pm j88.83$ $-59.62 \pm j83.30$ $-1.369 \pm j157.9$ $-0.016 \pm j157.9$ $J_1/J_L = 1.058$

Table 5 Eigenvalues and normalized performance index of case C examples

Example C1 (reduced-order LQG)	Example C2 (present method)	Example C3 [present method with Eq. (15)]
Gains $G = \lfloor 0.0264, -0.237, 0.842, 5.671, -22.54, 50.17 \rfloor$ $K = \lfloor 9.754, 39.41, 68.42, -1.470, -2.076, 56.60 \rfloor^T$ System eigenvalues $-2.025 \pm j9.898$ $-0.204 \pm j9.870$ $-14.31 \pm j41.57$ $-0.354 \pm j39.48$ $-2.025 \pm j98.98$ $-0.408 \pm j88.83$ $-0.003 \pm j157.8$ $J_1/J_L = 1.016$	Gains $G = \lfloor -0.0634, -0.0648, 0.952, 5.326, -22.52, 50.25 \rfloor$ $K = \lfloor 7.434, 33.12, 52.90, -5.698, 3.043, 44.92 \rfloor^T$ System eigenvalues $-0.192 \pm j9.867$ $-1.736 \pm j8.851$ $-12.03 \pm j42.37$ $-0.353 \pm j39.48$ -0.409 ± 88.83 $-46.57 \pm j92.15$ $-0.019 \pm j157.8$ $J_1/J_L = 1.015$	Gains $G = \lfloor -9.483, 1.576, 30.05, 87.58, -63.25, 130.9 \rfloor$ $K = \lfloor 2.242, 35.01, 93.01, -0.0033, -14.27, 64.13 \rfloor^T$ System eigenvalues $-3.172 \pm j9.035$ $-0.500 \pm j9.955$ $-0.950 \pm j39.30$ $-10.54 \pm j34.32$ $-1.065 \pm j88.95$ $-17.29 \pm j120.4$ $-0.500 \pm j157.6$ $J_1/J_L = 1.700$
Example C4 [present method with Eq. (16)]	**Example C5 (full-order LQG)**	
Gains $G = \lfloor -0.698, -1.294, 1.928, 28.13, -28.42, 50.70 \rfloor$ $K = \lfloor 4.487, 24.22, 49.33, -0.287, -2.422, 41.34 \rfloor^T$ System eigenvalues $-1.000 \pm j9.798$ $-1.000 \pm j10.08$ $-0.445 \pm j39.48$ $-9.218 \pm j39.99$ $-0.413 \pm j88.83$ $-41.09 \pm j97.29$ $-0.301 \pm j157.8$ $J_1/J_L = 1.016$	Gains $G = \lfloor 0.025, -0.211, 0.666, -1.384, 5.671, -22.54, 50.18, -87.18 \rfloor$ $K = \lfloor 9.754, 39.41, 68.42, 0.0, -1.470, -2.076, 56.60, 0.0 \rfloor^T$ System eigenvalues $-0.204 \pm j9.870$ $-2.026 \pm j9.897$ $-0.354 \pm j39.48$ $-14.33 \pm j41.61$ $-0.408 \pm j88.83$ $-59.62 \pm j83.30$ $-0.354 \pm j157.9$ $-0.016 \pm j157.9$ $J_1/J_L = 1.015$	

ues are not always associated with the same regulator or observer eigenvalues.

In order to compare the robustness of these examples, the values of modal stiffness $A_1(n_1+i,i)$, mode shapes at the actuator location $B_1(n_1+i,1)$, mode shapes at the sensor $C_1(1,n_1+i)$ of the controlled system, and the gains are varied up to $\pm 10\%$ independently, and the maximum increment of the normalized performance index is estimated. The results are listed in Table 3, where the normalizing value J_L is the performance index of LQR controller, which is estimated by

$$J_L = \mathrm{tr}[P_L V_{11}] \tag{19}$$

where P_L is the solution of

$$P_L A_1 + A_1^T P_L + Q_{11} = 0 \tag{20}$$

Table 3 indicates that these three configurations are identical

in robustness, which suggests that we do not have to worry which configuration is obtained. Although this is not guaranteed in cases with residual modes, we will not worry about the plural optima in the following examples with residual modes.

The regulator and the observer are designed through the present approach for all other cases of Table 1, which have the residual modes. Tables 4 and 5 list the gains, the eigenvalues, and the performance index of the resulting systems. For each example listed in the tables, the left column lists the eigenvalues of the regulator and the right column lists those of the observer. The bottom eigenvalues are those of the residual modes. The results of sensitivity analysis, where both the parameters of controlled modes and those of residual modes [i.e., $A_2(n_2+i,i)$, $B_2(n_2+i,1)$, and $C_2(1,n_2+i)$] are varied, are listed in Table 6. The value listed in the brackets following the infinity symbol ∞ indicates the margin to the instability boundary from the original values.

The LQG controller, whose order is the same as the controller to be designed by the present approach, is referred to as a "reduced-order" LQG controller in this paper. Example B1 is the case of a reduced-order LQG controller, which is designed by neglecting the residual modes. The positive real parts of the eigenvalues indicate the spillover instability, which is the same result as Ref. 15. Examples B2 and B3 are results of the present approach, with different parameter values of iteration termination condition for the NEWSUMT-A program. Although the values of J_1 in these two examples are almost identical, some gains and their eigenvalues are substantially different. Table 6 indicates that example B2 is almost on the instability boundary, particularly for observer gain variations (although much better than the unstable example B1). On the other hand, example B3 is very robust. This fact suggests not only a potential danger in the present approach in some ill-conditioned cases, but also that some eigenvalues can be shifted if they are left in the complex plane without substantially increasing J_1. The high sensitivity of example B2 seems due to its eigenvalue very close to the imaginary axis of the complex plane, -0.002. If this is true, the application of Eqs. (15) or (16) would be a good countermeasure to increase the stability margin. Example B4 is the result of the present approach using constraint [Eq. (15)], with $r^* = -0.5$. Example B5 is obtained by using the objective function [Eq. 16)], with $r^* = -1.0$ and $\epsilon = 0.01$. The eigenvalues have indeed been shifted left in the complex plane by these modifications as originally expected, without substantially increasing J_1. As expected, Table 6 indicates that examples B4 and B5 are considerably insensitive. Example B6 is the case of a full-order LQG controller, which controls all the n_1+n_2 modes. Table 4 indicates that the performance index J_1 of examples B2–B5, which are reduced-order controllers designed through the present approach, are almost identical with the value of the full-order LQG controller. Table 6 indicates that example B6 is not robust because only a 0.06% increment of the 4th mode stiffness causes instability, in spite of full-order feedback.

Case C, shown in Table 1, is the same as case B, except that $R = 3$. For the case of the reduced-order LQG controller (example C1), the eigenvalues listed in Table 5 show that it is stable, unlike case B. However, Table 6 indicates that it is relatively close to the instability boundary. Example C2 is designed by the present approach without any constraints. Although the improvement in the performance index J_1 is negligible in comparison with example C1, Table 6 indicates a large improvement in stability margin. Example C3 is obtained by the present method with constraint [Eq. (15)]. Unlike case B, a large penalty is required to force the real parts of the eigenvalues less than -0.5. In spite of this penalty, Table 6 indicates that example C3 is more sensitive than example C2. This example suggests that a lower value of the maximum real part of eigenvalues does not necessarily guarantee the insensitivity to the parameter variations. Example C4 is obtained by using the objective function [Eq. (16)], with $r^* = -1$ and $\epsilon = 0.01$. Tables 5 and 6 indicate that the degradation in J_1, due to the application of Eq. (16),

Table 6 Increment of normalized performance index ($\Delta J_1/J_L$) due to $\pm 10\%$ parameter variations

Example	B2	B3	B4	B5	B6	C1	C2	C3	C4	C5
Original J_1/J_L	1.0614	1.0613	1.0839	1.0641	1.0580	1.0164	1.0150	1.7000	1.0163	1.0147
Parameters										
A1(4,1) or A1(5,1)	0.0	0.0	0.0002	0.0	0.0	0.0	0.0	0.0001	0.0	0.0
A1(5,2) or A1(6,2)	0.0042	0.0043	0.0064	0.0037	0.0046	0.0033	0.0033	0.0158	0.0050	0.0033
A1(6,3) or A1(7,3)	0.0358	0.0353	0.0338	0.0319	0.0332	0.0334	0.0356	0.2570	0.0361	0.0338
A2(2,1) or A1(8,4)	0.0024	0.0023	0.0027	0.0014	∞(0.06%)	∞(−2.4%)	0.0005	0.0029	0.0002	∞(0.07%)
B1(4,1) or B1(5,1)	0.0	0.0	0.0	0.0	0.0	0.0	0.0	0.0002	0.0	0.0
B1(5,1) or B1(6,1)	0.0046	0.0046	0.0047	0.0046	0.0046	0.0048	0.0047	0.0073	0.0048	0.0048
B1(6,1) or B1(7,1)	0.1054	0.1054	0.1053	0.1053	0.1054	0.1036	0.1036	0.1565	0.1036	0.1036
B2(2,1) or B1(8,1)	0.0003	0.0003	0.0005	0.0002	0.0	0.0022	0.0	0.0008	0.0	0.0
C1(1,4) or C1(1,5)	0.0	0.0	0.0	0.0	0.0	0.0	0.0	0.0003	0.0	0.0
C1(1,5) or C1(1,6)	0.0008	0.0009	0.0010	0.0007	0.0009	0.0004	0.0003	0.0069	0.0012	0.0004
C1(1,6) or Cl(1,7)	0.0077	0.0077	0.0062	0.0074	0.0080	0.0057	0.0058	0.1383	0.0050	0.0059
C2(1,2) or C1(1,8)	0.0002	0.0001	0.0	0.0001	0.0	0.0015	0.0	0.0007	0.0	0.0
G(1,1)	∞(5.9%)	0.0	0.0	0.0001	0.0	0.0	0.0	0.0002	0.0	0.0
G(1,2)	0.0	0.0	0.0002	0.0002	0.0	0.0	0.0	0.0002	0.0	0.0
G(1,3)	0.0001	0.0	0.0004	0.0004	0.0	0.0001	0.0	0.0139	0.0	0.0
G(1,4)	—	—	—	—	0.0	—	—	—	—	0.0
G(1,4) or G(1,5)	∞(−4.3%)	0.0	0.0003	0.0003	0.0	0.0	0.0	0.0027	0.0	0.0
G(1,5) or G(1,6)	∞(5.0%)	0.0	0.0006	0.0004	0.0003	0.0006	0.0002	0.0071	0.0010	0.0002
G(1,6) or G(1,7)	∞(−6.9%)	0.0054	0.0091	0.0054	0.0053	0.0099	0.0051	0.1290	0.0050	0.0052
G(1,8)	—	—	—	—	0.0	—	—	—	—	0.0
K(1,1)	∞(−3.9%)	0.0002	0.0002	0.0002	0.0	0.0001	0.0	0.0004	0.0	0.0
K(2,1)	∞(5.2%)	0.0	0.0032	0.0011	0.0001	0.0001	0.0	0.0144	0.0	0.0
K(3,1)	∞(−6.8%)	0.0	0.0021	0.0001	0.0002	∞(3.9%)	0.0001	0.0084	0.0002	0.0001
K(4,1)	—	—	—	—	0.0	—	—	—	—	0.0
K(4,1) or K(5,1)	∞(0.01%)	0.0	0.0	0.0	0.0	0.0	0.0	0.0	0.0	0.0
K(5,1) or K(6,1)	∞(−0.02%)	0.0002	0.0009	0.0005	0.0	0.0	0.0	0.0036	0.0	0.0
K(6,1) or K(7,1)	∞(−0.03%)	0.0006	0.0045	0.0010	0.0002	0.0004	0.0	0.0018	0.0	0.0
K(8,1)	—	—	—	—	0.0	—	—	—	—	0.0

is negligible and that the resulting configuration is insensitive. Example C5 is the full-order LQG controller. There is no advantage of this full-order controller, since it is almost on the instability boundary and the improvement in J_1 is negligible.

Figure 2 plots the values of the response index vs normalized control effort C_E/R for various values of R. All the other parameter values are the same as cases B and C. The solid line indicates the result of the present approach; the broken line indicates that of the reduced-order LQG controller. The figure indicates that the reduced-order LQG controller cannot reduce the value of response index γ as much as the controller designed by the present approach. The figure also indicates that the performance of the reduced-order LQG controller is almost identical with the present controller only when the value of R is larger than 3.

Finally it should be noted that the stability of the reduced-order controller (i.e., $n_2 = 0$) is not always guaranteed. In fact, the present approach fails to design a stable system in the case of $n_1 = 3$, $n_2 = 2$, $\zeta = 0$. So far as investigated above, however, we can conclude that the present approach, especially the approach with Eq. (16), can result in an excellent controller in many cases, which is superior or the same compared with not only the reduced-order LQG controller neglecting the residual modes but also the full-order LQG controller.

Integrated Optimization of Structure, Regulator, and Observer

The preceding optimization approach of regulator and observer can be easily incorporated with the structural optimization into an integrated optimization approach, because the structural optimization already requires a numerical nonlinear optimization technique.

The requirement for the spacecraft structure and its controller to maintain the structural shape and attitude with a given accuracy, as presented in Ref. 4, is used in this investigation. This condition requires the amplitude of the response (γ) due to the given disturbance (w_{11}, w_{12}, w_2) less than a certain allowable limit (γ^*). The objective function to be minimized is the total cost of the structure and the controller in a wide sense. In the present investigation, the total cost is approximated by

$$J_2 = \alpha C_E + (\text{normalized structural mass}) \tag{21}$$

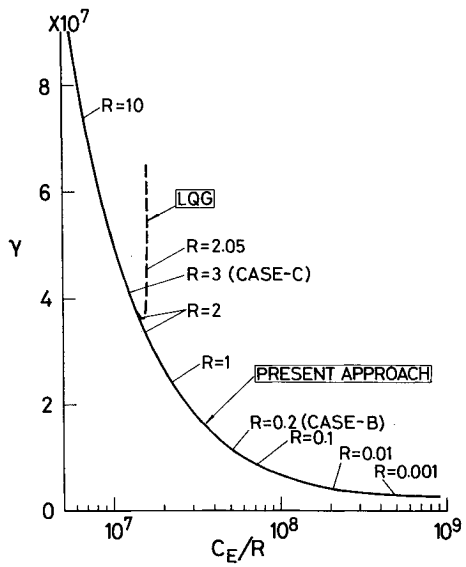

Fig. 2 Response index and control effort C_E for various values of R.

where the constant value of α reflects the cost of the control system. The first term on the right-hand side of Eq. (21) represents the control cost; the second one represents the structural cost. Therefore, the present integrated optimization problem is to find the values of G and K, and the structural parameters that minimize J_2 with the constraint, such that

$$g_2 \equiv \gamma^* - \gamma \geq 0 \tag{22}$$

It should be noted that the effect of the residual modes is taken into account because γ and C_E are defined by Eqs. (1–5), (7), and (8). Because of the residual modes, the nesting optimization scheme,[4] which takes advantage of the LQG or LQR approach, cannot be used to solve this optimization problem; therefore, the direct numerical optimization approach is used.

It would be a good scheme to modify the objective function in the same manner as Eq. (16), in order to reduce the real parts of the eigenvalues by

$$J_2' = \left\{1 + \epsilon \sum_i h[\mathrm{Re}(\lambda_i) - r^*]\right\} J_2 \tag{23}$$

Beam-Like Spacecraft Example

In order to demonstrate the present approach, the structure, the regulator, and the observer of a beam-like spacecraft, shown in Fig. 3, are optimized as an example. The spacecraft is symmetric and a uniformly distributed payload, whose mass per unit length is ρ_P, is supported by the structure. A torque actuator and an angle sensor are installed at the center. The control system is the same as Eqs. (3–5). The control force u is a torque, and the output y is an angular signal in this example. The cross-sectional area of the structure is assumed to be a piecewise-constant function over constant intervals. The total mass per unit length at the ith interval is

$$\rho_i = \rho_P(1 + \xi_i) \tag{24}$$

where ξ_i is the normalized cross-sectional area at the ith interval. The bending stiffness at the ith interval is assumed to be

$$EI_i = EI_N \xi_i \tag{25}$$

The structure is subjected to a disturbance force

$$f_D(X,t) = \sqrt{3}(X/L)\rho(X) f_w(t) + (|X| - L)\,\mathrm{sign}(X) f_t(t) \tag{26}$$

where

$$\mathrm{sign}(z) = \begin{cases} 1 & \text{if } z \geq 0 \\ -1 & \text{if } z < 0 \end{cases} \tag{27}$$

and

$f_w(t)$ = white noise whose intensity is V_w

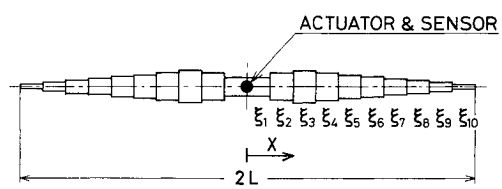

Fig. 3 Free-free beam approximating a spacecraft.

$f_t(t)$ = noncorrelated white noise whose intensity is $0.01V_w$

$\rho(X)$ = total mass per unit length

X = coordinate along the spacecraft with the origin at its center

The second term on the right-hand side of Eq. (26) is introduced in order to avoid the unique situation where the disturbance is orthogonal with all of the vibration modes. Because the spacecraft is symmetric and the disturbance is antisymmetric, only the antisymmetric modes of one-half structure need to be investigated.

The total cost for this example is approximated by

$$J_2 = \alpha C_E + \sum_i^{n_s} \xi_i / n_s \tag{28}$$

The optimization problem of this example is to find the values of G, K, and ξ_i, that minimize J_2 or J_2' with the constraint [Eq. (22)].

The values of Q_{11} and Q_{22} are selected such that γ represents the mean square of displacement. In addition, the following values are used for various parameters:

$$n_1 = 3, \quad n_2 = 2, \quad R = 1, \quad \bar{V}_2 = 10^{-3}, \quad \xi = 10^{-3}$$
$$\bar{\gamma}^* = 0.05, \quad \bar{\alpha} = 0.1, \quad n_s = 10$$

where

$$\bar{\gamma}^* \equiv \gamma^* EI_N^{3/2} \rho_P^{1/2} / (V_w L^6)$$
$$\bar{\alpha} \equiv \alpha V_w L^5 EI_N^{1/2} / \rho_P^{3/2}$$
$$\bar{V}_2 \equiv V_2 EI_N^{3/2} \rho_P^{1/2} / (V_w L^4) \tag{29}$$

Each interval of the structure through which the bending stiffness and the density are constant is simulated by a standard Euler beam finite element with cubic shape function.

Table 7 shows the costs, response index, and normalized eigenvalues of the results of the present structure/controller integrated optimization approach. Example D1 is obtained by using the objective function [Eq. (28)]; example D2 is obtained by using the modified objective function [Eq. (23)], with $r^* = -0.5$ and $\epsilon = 0.05$. Several local optima with substantially different values of J_2 are obtained by using different initial values, unlike the almost identical value of J_2 for the simply supported beam examples. However the table only shows the best case for J_2, which is obtained by using the rounded values of the results of another optimization as the initial values. The comparison of the examples indicates that the real parts of all the eigenvalues, except for a tough pair, have been reduced to less than r^* by the modification of the objective function. The penalty for this reduction is a 18% increase in J_2. Table 8, which lists the sensitivity, shows that example D2 is more robust and has a larger stability margin than example D1. The optimal distribution of structural cross-sectional areas of the examples are plotted in Fig. 4. These examples demonstrate that the present integrated direct optimization approach works well and results in an excellent design.

The separate sequential optimizations are also carried out, based on the objective function [Eq. (28)] and the constraint [Eq. (22)], in order to investigate the advantage of structure/controller simultaneous optimization. In the sequential optimization, the controller gains are first optimized, and then, separately, the structures are optimized. The total cost results J_2 are plotted in Fig. 5, where the symbols S and G indicate the optimization with respect to the structure only and the control gains only, respectively. The initial values for the gains are those of the reduced-order LQG controller, and the initial values for the structural parameters are unity. It can be seen that the separate optimization of the structure and controller is not very effective. The figure shows that the total

Table 7 Costs and eigenvalues of beam-like spacecraft designed by the present approach

	Example D1	Example D2
Total cost (J_2)	0.239	0.283
Structural cost	0.122	0.151
Control cost (αC_E)	0.116	0.132
Response index (γ)	0.500	0.500
Eigenvalues	$-1.024 \pm j1.090$	$-1.937, -11.02$
	$-1.796 \pm j3.450$	$-1.242 \pm j1.487$
	$-0.521 \pm j5.165$	$-0.670 \pm j4.720$
	$-1.067 \pm j6.095$	$-0.500 \pm j6.591$
	$-1.842 \pm j11.27$	$-2.645 \pm j11.53$
	$-0.283 \pm j15.30$	$-0.559 \pm j16.26$
	$-0.012 \pm j32.37$	$-0.500 \pm j35.78$
	$-0.008 \pm j53.70$	$-0.354 \pm j59.49$

Table 8 Increment of J_2 and γ due to $\pm 5\%$ parameter variations

	Example D1		Example D2	
	J_2	γ	J_2	γ
Original value	0.239	0.500	0.283	0.500
	ΔJ_2	$\Delta\gamma$	ΔJ_2	$\Delta\gamma$
Parameters				
A1(4,1)	0.0	0.0	0.0	0.0
A1(5,2)	∞	∞(2.7%)	0.020	0.127
A1(6,3)	0.008	0.008	0.016	0.008
A2(3,1)	0.001	0.003	0.001	0.004
A2(4,2)	0.001	0.002	0.0	0.002
B1(4,1)	0.0	0.041	0.003	0.043
B1(5,1)	0.007	0.022	0.009	0.021
B1(6,1)	0.002	0.006	0.001	0.006
B2(3,1)	0.001	0.004	0.001	0.004
B2(4,1)	0.001	0.002	0.001	0.002
C1(1,4)	0.007	0.038	0.008	0.041
C1(1,5)	0.006	0.019	0.008	0.019
C1(1,6)	0.001	0.006	0.001	0.006
C2(1,3)	0.001	0.004	0.001	0.004
C2(1,4)	0.001	0.002	0.0	0.002
G(1,1)	0.003	0.009	0.003	0.009
G(1,2)	0.007	0.023	0.012	0.030
G(1,3)	0.014	0.044	0.016	0.043
G(1,4)	∞	∞(3.1%)	0.004	0.020
G(1,5)	0.0	0.0	0.001	0.002
G(1,6)	∞	∞(−3.6%)	0.002	0.011
K(1,1)	0.0	0.001	0.001	0.003
K(2,1)	0.001	0.002	0.001	0.001
K(3,1)	0.0	0.0	0.0	0.002
K(4,1)	∞	∞(3.1%)	0.001	0.006
K(5,1)	0.0	0.0	0.0	0.0
K(6,1)	∞	∞(−4.0%)	0.005	0.002

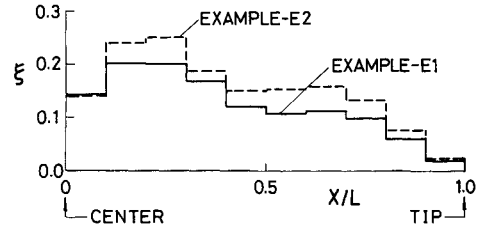

Fig. 4 Optimal distribution of structural cross-sectional area.

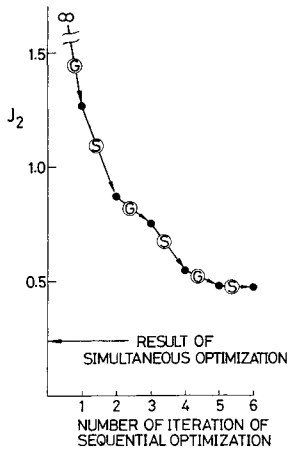

Fig. 5 Total cost of the results of separate sequential optimization.

Table 9 Eigenvalues of the system designed without taking into account residual modes

Without residual modes	With residual modes
-0.707 ± 1.092	$-1.933, -20.75$
-0.246 ± 4.132	-0.801 ± 1.327
-1.554 ± 4.495	-0.507 ± 4.510
-0.718 ± 5.190	-0.461 ± 5.408
-0.034 ± 13.10	-0.048 ± 13.75
-0.153 ± 13.46	-0.538 ± 14.28
——	1.915 ± 31.29
——	1.714 ± 50.04

cost of the result of separate sequential optimization is much higher than that of simultaneous optimization even after the several iterations, demonstrating the advantage of the simultaneous optimization.

The effect of residual modes on the optimal design of the structure and controller are investigated by, first, optimizing the structure and controller without taking into account the residual modes (i.e., $n_1 = 3$, $n_2 = 0$), and, second, estimating the characteristics of the resulting system, taking account of the residual modes. The left column of Table 9 lists the eigenvalues of the resulting system estimated without any residual modes; the right column of the table lists the eigenvalues estimated with the inclusion of two residual modes into the mathematical model. The table shows that the effects of the residual modes are significant and that the system optimized without taking into account the residual modes is unstable due to the spillover. This example demonstrates the necessity of taking into account the residual modes in the optimal design of the structure and controller.

The integrated optimization of structure and the reduced-order LQG controller is also tried by using various initial values. However, it fails to obtain any feasible configuration that satisfies Eq. (22), which demonstrates the advantage of the present approach.

The integrated optimization with full-order (i.e., $n_1 = 5$, $n_2 = 0$) LQG controller resulted in a J_2 value of 0.177, which is 26% better than that of the result of the present approach. However, it is very close to the instability boundary, and a 0.5% reduction of the stiffness of the fifth mode leads to an instability.

Finally, it should be noted that the present approach has been shown to work well for the simple examples with a relatively small number of design parameters. Further improvement is still required to apply it to complex systems because the present direct optimization approach increases the number of design parameters, and the nonlinear optimization scheme would require a huge amount of computation when the number of the design parameter is large.

Conclusions

A direct numerical optimization approach, which takes into account the uncontrolled residual modes, is proposed for the integrated structure/regulator/observer optimization problem. The approach is applied to the optimal design of the controller of a simply supported beam, and the characteistics of the resulting controller are studied. Through various examples, the following conclusions are obtained.

1) The present approach results in a higher performance controller than a reduced-order LQG controller degraded by spillover. It results in a stable system even when the reduced-order LQG controller is unstable due to spillover.

2) The controller designed through the present approach, especially with the modified objective function, is less sensitive to the parameter variation than the LQG controller. It is even less sensitive than a full-order LQG controller in some cases.

Subsequently, the direct optimization approach of the controller is incorporated in the integrated structure/controller optimization scheme, and applied to a free-free beam-like spacecraft example. From the results of this numerical investigation, the following conclusions are also obtained.

1) The present integrated optimization approach results in a robust, stable, and high-performance system even when an integrated optimization using the reduced-order LQG controller cannot find even a feasible configuration.

2) The integrated direct optimization can result in an unstable system unless the residual modes are taken into account, as in the present approach.

3) The present approach works well and its effectiveness has been demonstrated.

Since the present examples are limited to a relatively small number of simple examples, further studies on the characteristics of the resulting system are required as future work. Reduction of the computational effort for the present approach is also left for further work.

References

[1]Hale, A. L., Lisowski, R. J., and Dahl, W. E., "Optimal Simultaneous Structural and Control Design of Maneuvering Flexible Spacecraft," *Journal of Guidance, Control, and Dynamics*, Vol. 8, Jan.–Feb. 1985, pp. 86–93.

[2]Bodden, D. S., and Junkins, J. L., "Eigenvalue Optimization Algorithms for Structure/Controller Design Iterations," *Journal of Guidance, Control and Dynamics*, Vol. 8, Nov.–Dec. 1985, pp. 697–706.

[3]Messac, A., Turner, J., and Soosaar, K., "An Integrated Control and Minimum Mass Structural Optimization Algorithm for Large Space Structures," *Proceedings of JPL Workshop on Identification and Control of Flexible Space Structures*, Jet Propulsion Laboratory, Pasadena, CA, JPL Publication 85-29, Vol. II, April 1985, pp. 231–266.

[4]Onoda, J., and Haftka, R. T., "An Approach to Structure/Control Simultaneous Optimization for Large Flexible Spacecraft," *AIAA Journal*, Vol. 25, No. 8, 1987, pp. 1133–1138.

[5]Khot, N. S., Grandhi, R. V., and Venkayya, V. B., "Structural and Control Optimization of Space Structures," *Proceedings of the AIAA/ASME/ASCE/AHS 28th Structures, Structural Dynamics, and Materials Conference*, AIAA, NY, April 1987.

[6]Hale, A. L., "Integrated Structural/Control Synthesis via Set-Theoretic Methods," *Proceedings of the AIAA/ASME/ASCE/AHS 26th Structures, Structural Dynamics, and Materials Conference*, AIAA, NY, April 1985.

[7]Lust, R. V., and Schmit, L. A., "Control-Augmented Structural Synthesis," *AIAA Journal*, Vol. 26, No. 1, 1988, pp. 86–95.

[8]Belvin, W. K., and Park, K. C., "Structural Tailoring and Feedback Control Synthesis: An Interdisciplinary Approach," *Proceedings of the AIAA/ASME/ASCE/AHS 29th Structures, Structural Dynamics, and Materials Conference*, AIAA, New York, April 1988.

[9]Rao, S. S., Venkayya, V. B., and Khot, N. S., "Game Theory Approach for the Integrated Design of Structures and Controls," *AIAA Journal*, Vol. 26, No. 4, 1988, pp. 463–469.

[10]Balas, M. J., "Active Control of Flexible Systems," *Journal of Optimization Theory and Applications*, Vol. 25, No. 3, July 1978, pp. 415–436.

[11]Kosut, R. L., "Suboptimal Control of Linear Time-Invariant System Subject to Control Structure Constraints," *IEEE Transactions and Automatic Control*, Vol. AC-15, No. 5, Oct. 1970, pp. 557–563.

[12]Thareja, R., and Haftka, R. T., "NEWSUMT-A: A General Purpose Program for Constrained Optimization Using Constraint Approximations," *ASME Journal of Mechanics, Transmission and Automation in Design*, Vol. 107, March 1985, pp. 94–99.

[13]Kwakernaak, H., and Sivan, R., *Linear Optimal Control System*, Wiley-Interscience, NY, 1972.

[14]Onoda, J., "An Attempt for Simultaneous Structure/Control Optimization of Large Flexible Spacecraft," *Proceedings of the Pacific Basin International Symposium on Advances in Space Science Technology and Its Applications*, June 1987, pp. 549–557.

[15]Czajkowski, E. A., and Preumont, A., "Spillover Stabilization and Decentralized Modal Control of Large Space Structures," AIAA Paper 87-0903, April 1987.